Effect of Carbon Addition and Sintering Temperatures on Densification and Microstructural Evolution of Sinter-Hardening Alloy Steels

Neerav Verma and Saurabh Anand

Department of Materials & Metallurgical Engineering
Indian Institute of Technology, Kanpur, India 208016

Abstract

The iron-copper-carbon alloys are used extensively in powder metallurgy due to their superior dimensional control; however, they possess lower mechanical properties, corrosion resistance and wear resistance than their wrought counter part. In recent years, there have been concerted attempts to engineer ferrous alloys with high dimension tolerance and enhanced mechanical properties. One such approach is to use prealloyed iron powder instead of pure iron, mixed with copper and carbon. SH737-2Cu-C is one such alloy. The present study focuses on the effect of carbon addition on diffusion of Cu in SH737 alloys system via microstructural studies. SH737-2Cu alloys were compacted, sintered and characterized. The materials were characterized according to their density, densification parameter, shape factor, and pore size distribution. The microstructural studies revealed bimodal pore distribution in the sample with no carbon, due to the presence of primary and secondary porosity. The shape factor distribution showed more roundedness in the case of carbon added alloys. The size of the primary pores depends on compaction pressure and powder size distribution. On the other hand, size and morphology of the secondary pore strongly depends on Cu powder size, its homogeneity and sintering temperature. Also, an increase in the sintering temperature increased the roundedness and the pores became coarser.

Keywords: Transient liquid phase sintering, SH737-2Cu alloys, shape facto, pore size, distribution, pore coarsening, primary and secondary pores

1. Introduction

In recent years, ferrous alloys processed using the powder metallurgy (P/M) route have been used extensively in automobile applications. P/M has become a preferred route over other manufacturing processes for a variety of reasons: P/M offers economic advantages, ease in the manufacturing of small-sized pieces with complicated shapes, high dimensional accuracy, greater material utilization (>95%), and flexibility to tailor the composition and engineer the microstructure.[1] P/M products also have greater microstructural homogeneity. The significant advances in powder production technology, new alloy design with novel properties, compaction, and sintering furnace technologies have boosted the growth of powder metallurgy.

Alloying methods of iron are divided into groups: admixed powders, partially prealloyed powder, hybrid powder and coated powder. In furnace alloys, typical alloying additions include Ni, Mo, Mn, Cr, Cu and C. Most of these alloying additions enhance the strength through solid solution hardening during sintering. In addition, these alloying additions also enhance the hardenability by shifting the continuous cooling transformation curve to the right. Subsequent heat treatment results in enhancing the toughness of ferrous alloys.

One of the most common alloying elements used in ferrous powder metallurgy is copper. The use of copper in ingot metallurgy is restricted to weathering steel only. In P/M, because of its low melting point, copper is known to activate sintering at low temperature, which ensures homogeneous mixing of the powder. Presence of copper during liquid phase sintering

results in compact swelling. his phenomenon has been mostly observed and extensively investigated in steels containing less than 20 wt% Cu.[2-6] Kayesser *et al.*[6] determined that the molten copper penetration through grain boundaries is the greatest contributor to the swelling phenomenon. It has been observed that compact swelling can be compensated for by the addition of carbon in steels. Dilatometric studies of Fe-C-Cu found that the large expansion associated with the copper growth phenomenon decreases with increasing carbon content.[7-9] Originally this beneficial effect of carbon was attributed to the reduction of Cu solubility in iron and development of a liquid phase.

For the last few decades, there has been an increased desire to use powder metallurgy products as structural components. Structural components require a high relative density for excellent mechanical properties and therefore must have low porosity.[10] A pore acts as a stress concentrator and plays an important role in material failure. The role of porosity on mechanical and physical properties of sintered materials has been studied frequently.[11-14] Formation of secondary pores at the site of original Cu particles is an inevitable consequence of transient liquid phase sintering; therefore, these sintered steels contain numerous largely spherical secondary pores in addition to the pores originating from the green compact. Tina M. Cimino and others observed that mechanical properties of FC-0205 and FC-0208 steels improved with increasing sintering temperature, which is due to the difference in pore morphology and different diffusion mechanism of Cu and Ni during the sintering process. Many researchers observed that copper particle size has no significant effect upon final pore shape.[15-17] The current study was designed to provide quantitative metallography data to understand pore size distribution and the change in pore morphology with different sintering temperatures.

Transient liquid phase sintering of low copper based steel (<9% Cu) forms small secondary pores due to transient liquid formation and large primary pores due to packing characteristic of the powder and binder burn out. In addition to these residual pores, ferrous P/M steels exhibit heterogeneous microstructures due to inhomogeneous distribution and incomplete diffusion of alloying elements. The influence of chemical and microstructural homogeneity on the mechanical properties of sintered material has been studied by a number of researchers.

This study focuses on the investigation of one such alloy SH737 (designated) which has a nominal composition of Fe-1.25 Mo-1.4 Ni-0.42 Mn (wt%). This grade of powder has also been referred as sinter-hardening grade, which achieves sintering and hardening in a single step.

2. Experimental Procedure

For the present investigation, two partially prealloyed powder mixtures, (a) and (b), were made by a proprietary process developed by Hoeganaes Corp viz.[18-19]

(a) Fe, 1.4 wt % Ni, 1.25 wt % Mo, 0.42 wt % Mn, 2 wt % Cu or SH737-2Cu

(b) Fe, 1.4 wt % Ni, 1.25 wt % Mo, 0.42 wt % Mn, 2 wt % Cu, 0.9 wt % C or SH737-2Cu-0.9C

The as received powder was characterized for its flow behavior, apparent, and tap density using set MPIF standards. The results are tabulated in Tables 1 and 2. The cumulative weight percent of the powder particles vs. particle size is displayed in Figure 1. A SEM image of the powder used for sample preparation is shown in Figure 2.

Powders were pressed at 600 MPa in a 50 ton uniaxial hydraulic press (APEX construction Ltd, UK). Densities of the compacted specimens were between 6.99 and 7.02 g/cm^3. To minimize friction, the compaction was carried out using zinc stearate as a die wall lubricant. The powder contains 0.75 wt.% acrawax, which was added to the powder to facilitate its compaction during sintering. The sintering response on densification

Table 1. Composition of the powder

Elements	Fe	Mo	Mn	Ni	Cu	C
% (by wt)	94.03	1.25	1.4	0.42	2	0.9

Table 2. Characteristics of experimental powder

Source	D_{10} (µm)	D_{50} (µm)	D_{90} (µm)	Mode size, (µm)	Width of distribution (µm)	Apparent Density, (g/cm^3)	Tap Density, (g/cm^3)	Flow Time, (s/50g)
Hoeganaes	32	58	88	75	0.47	3.62	3.98	20

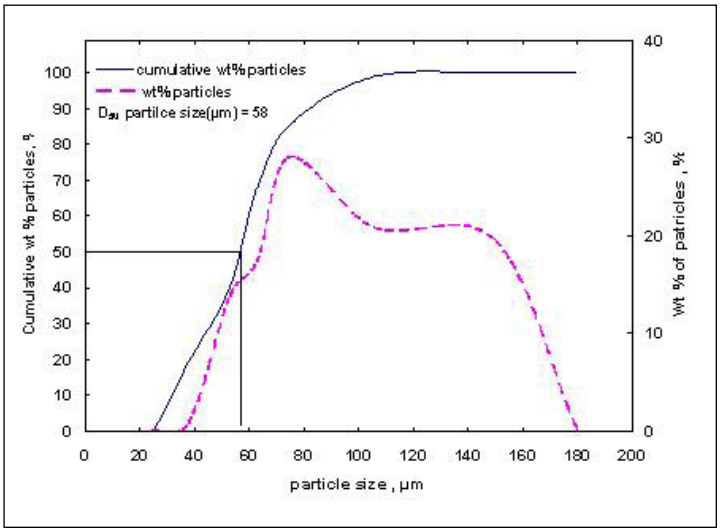

Figure 1. Cumulative weight % of the powder particles vs particle size

and microstructures were evaluated on cylindrical pellets (16 mm diameter and 6 mm height). The wax was removed from the green compacts in a tubular silicon carbide (SiC) furnace under N_2-20% H_2 atmosphere. The lubricant was removed from the green samples using a heat treatment at 850 °C for 30 min. To prevent cracking of green compacts by thermal shock, the green samples were heated at 3 °C/min. Then the compacts were sintered at two different temperatures, 1120 °C and 1180 °C, for 30 min in a tube furnace with SiC heating elements. The thermal profiles for the sintering are shown in Figure 3. All the sintering was carried out under N_2-20% H_2 atmosphere.

The sintered density was obtained by dimensional measurements. The densification parameter was calculated to determine the amount of densification that occurred during sintering. It is expressed as:

$$\text{Densification parameter} = \frac{\text{(sintered density - green density)}}{\text{(theoretical density - green density)}} \quad (1)$$

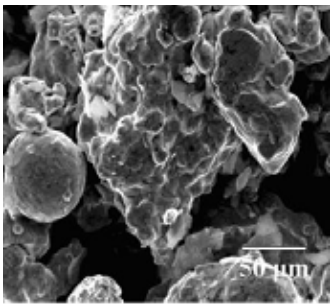

Figure 2. SEM image of the powder used for sample preparation

Standard metallographic practices were employed for sample preparation for microstructural examination. The sintered samples were mounted, with the help of epoxy, and wet polished in a manual polisher (model: Lunn Major, supplier: Struers, Denmark) using a series of SiC emery papers followed by cloth polishing using a suspension of 1 µm and 0.03 µm alumina.

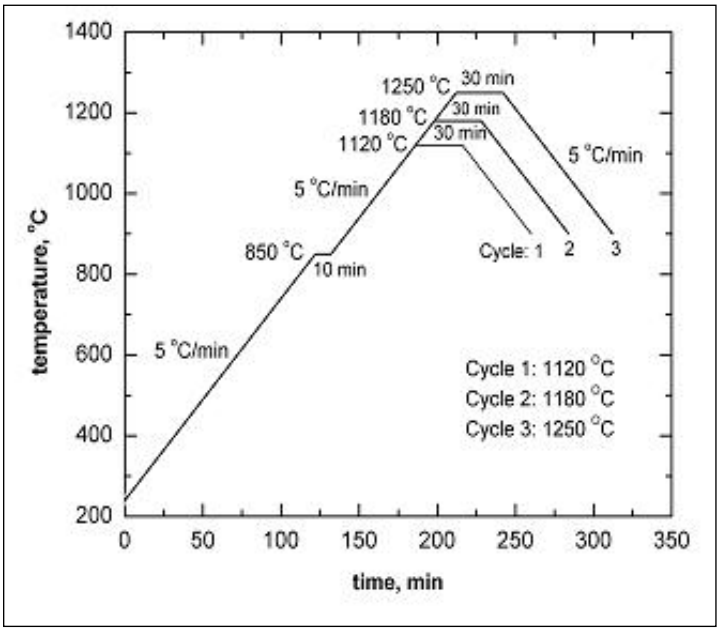

Figure 3. Sintering temperature profiles for SH737Fe-2Cu-0.9C for different temperatures

An optical microscope with digital image acquisition capability (model: LABORLUX 12 ME S, supplier: Leitz Germany) was used to obtain the micrographs of sintered polished samples. Pictures (20 at each sintering temperature) were taken randomly with an optical microscope at a magnification of 100X. The size of pores was measured manually with a precision of 1 mm. For each sample, more than 5,000 readings were taken in order to eliminate experimental errors and get statistically correct results.

At the same time, quantitative metallographic analysis was performed on the samples, according to standard pixel analysis method, on a calibrated image analysis system.

Some basic parameters were determined from quantitative analysis. A well-known and often used characteristic for particle irregularity characterization is roundness of the object (RN). It is defined as:[20,21]

$$RN = P^2/4\pi A \quad (2)$$

where P is the circumference and A is the area. The roundness of a circle is equal to one. If the object's shape approaches a line segment, it approaches infinity. To characterize the roundness, sometimes a shape factor SF=1/RN is used, where SF predicts the degree of irregularity. A shape factor equal to one represents a circular pore. As the number decreases from one, the degree of irregularity increases. The roundness factor proposed by Salek *et al.*[12] RFN is define by the relationship

$$RFN = P/d_A \quad (3)$$

where d_A is the diameter of the circle with the same area as the particle.

In addition to quantitative analysis of the unetched microstructure, optical microscopy was conducted on samples in the etched condition and the SF calculated.

3. Results and Discussion

The current study provides a quantitative metallography analysis protocol to understand pore size distribution and

Table 3. Average volume % of porosity for the sintered samples

Sintering Temperature(°C)	Pore Volume percent (%)	
	0% C	0.9% C
1120	11.75±0.67	12.52±0.84
1180	13.14±0.59	11.89±0.76

change in pore morphology with addition of carbon and different sintering temperatures for SH737-2Cu alloys.

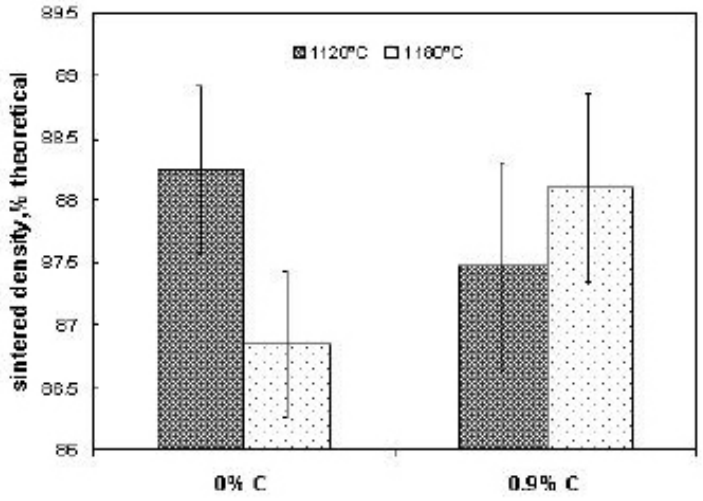

Figure 4. Effect of sintering temperature and carbon addition on sintered density (% theoretical) of SH737-2Cu system

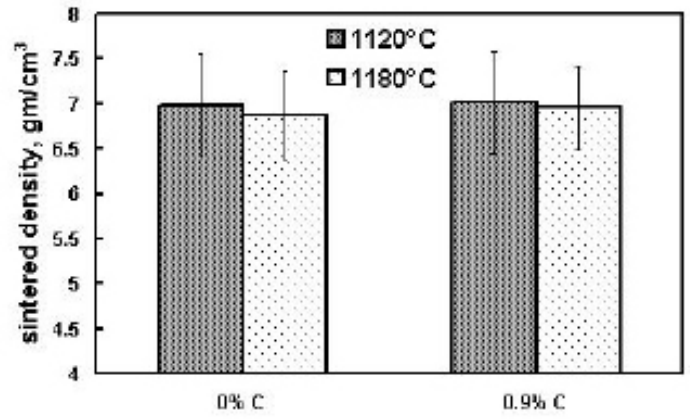

Figure 5a. Effect of sintering temperature and C addition on sintered density of SH737-2Cu system

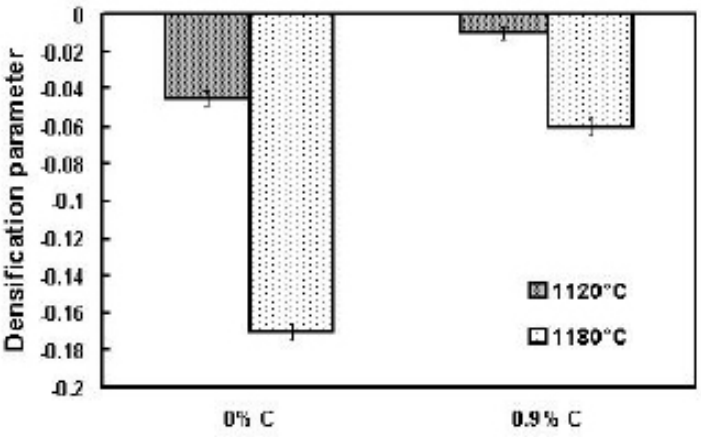

Figure 5b. Effect of sintering temperature and C addition on densification parameter of SH737-2Cu system

Cylindrical samples with green density of 6.98 ± 0.02 g/cm^3 were used for sinter density measurement and pore volume fraction calculation, as shown in Table 3. For all the cases, the volume fraction of pores lies between 11 and 14%. The total porosity was determined through quantitative image analysis.

The residual porosity after sintering may be characterized as either primary or secondary pores. Primary pores are large pores that result from geometric packing of the particles or from binder burn out. Secondary porosity is typically smaller in nature and may be attributed to residual porosity from liquid phase formation and diffusion of alloying addition, such as copper. Due to secondary pore formation, the sintered density is lower than the green density in this alloy. The effect of sintering temperature and carbon addition on sintered density (percent theoretical), in the SH737-2Cu system is shown in Figure 4. Figure 5a compares the effect of carbon and sintering temperature on the density of SH737-2Cu alloys. The sintering density varies marginally with sintering temperature and addition of carbon. Figure 5b shows the effect of sintering temperature and carbon addition on the densification parameter of the SH737-2Cu system.

The densification parameter gives an account of whether swelling or shrinkage is occurring in the sample. As can be clearly seen, in both cases we obtain swelling in the sample. In the absence of carbon, we obtain slight swelling due to the diffusion of copper. As the amount of carbon is increased, the sintered density is observed to rise and swelling is reduced.

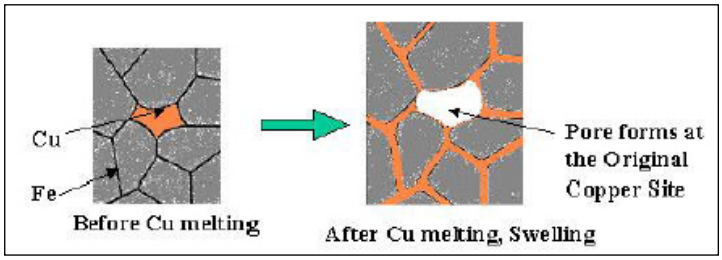

Figure 6. Process of transient liquid phase sintering resulting in the diffusion of copper, porosity, and swelling in sintered hardened samples

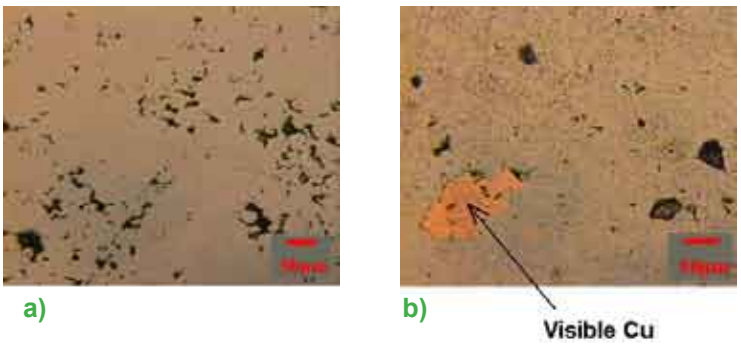

Figure 7. Optical microstructures of a) SH737-2Cu, b) SH737-2Cu-0.9C, showing absence of visible copper in case of SH737-2Cu due to Cu diffusion into the matrix of iron

More swelling corresponds to a more negative value of densification parameter, so more swelling was obtained for the sample without any carbon addition due to the free diffusion of the copper into the matrix as a result of transient liquid phase sintering. This can be seen in Figure 6 at 1120 and 1180 °C.

Carbon hinders "copper growth," preventing excessive penetration of copper rich liquid along grain boundaries or interparticle boundaries. Because of the increase in the dihedral angle between iron and copper, there was a reduction in swelling due to the carbon addition. This process of hindering of copper diffusion can be seen in Figure 7, where unalloyed metallic Cu can be seen at distinct places in optical microstructures in the case of 0.9% carbon addition.

Figure 8 shows the shape factor distribution of pores in samples SH737-2Cu and SH737-2Cu-0.9C at (a) 1120 °C and (b) 1180 °C as sintering temperatures. In case there was no carbon, we obtained a bimodal distribution because of two types of pores forming:

(a) Primary pores formed at the time of compaction process
(b) Secondary pores formed at the time of sintering process due to copper diffusion due to transient liquid phase sintering

In the case of 0.9% addition of carbon, the average SF approaches unity, i.e. more roundedness. This increase in roundness results from the contribution of pores, which is only due to compaction; therefore, more circular pores are obtained, implying relatively more roundedness of primary pores as compared to secondary pores.

In the case of no carbon addition, the average SF decreases. This decrease is now due to contribution of two things: firstly due to secondary pores, which are more irregular; secondly due to primary pores, which are relatively spherical and have shape factor value close to unity. We can then deduce that in the bimodal distribution, the right peak is for the primary pores

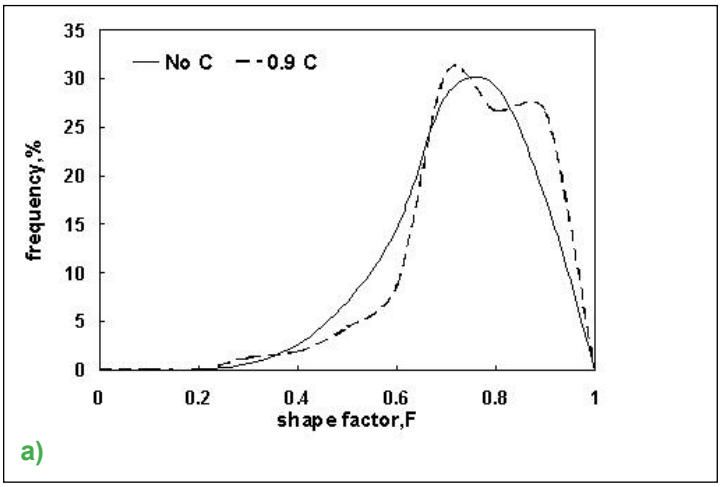

Figure 8. Variation of frequency % with shape factor of pores in samples SH737-2Cu and SH737-2Cu-0.9C at a) 1120 °C and b) 1180 °C as sintering temperatures

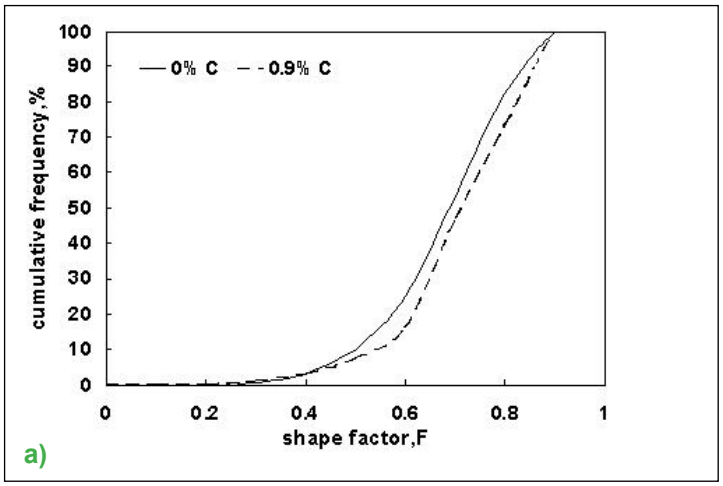

Figure 9. Cumulative frequency distribution of SH737-2Cu and SH737-2Cu-0.9C at a) 1120 °C and b) 1180 °C as sintering temperatures

showing more spherical nature of such pores, and the left peak is for the secondary pores which are relatively more irregular.

More average roundedness of pores (SF approaching to one) in the case of 0.9% carbon can clearly be seen from Figure 9, which shows cumulative frequency distribution of SH737-2Cu and SH737-2Cu-0.9C at sintering temperature of a) 1120 °C and b) 1180 °C. For both sintering temperatures, the plot of 0.9% C is consistently shifted to the right of 0% C plot, and thus more average roundedness in case of carbon addition.

Figure 10 shows the distribution of pore SF for different sintering temperatures (i.e. 1120 °C and 1180 °C) for (a) SH737-2Cu and (b) SH737-2Cu-0.9C. The SF gives a quantitative measure of pore morphology. A SF equal to one represents a circular pore in the plane of analysis, and as the number decreases from one, the degree of irregularity increases. The shape analysis graph shows that pores at 1120 °C sintered samples are more irregular. With an increase in temperature, the peak of the graphs shift marginally towards the right side for both (a) and (b); therefore, overall irregularity of the mass of pores decreases with increasing sintering temperature. Because the SF is a ratio of pore area and pore perimeter, the frequency vs. SF plot does not predict the effect of pore size on SF.

Figure 11 shows the effect of pore size on SF. From this figure, it is obvious that pores below 100 μm² have a SF between 0.3 and 0.85. It is also clear from this figure that pores in this range have a wide distribution in shape. Furthermore, results indicate that pores above 100 μm² are more irregular and have a SF from 0.4 to 0.15. It can also be seen that at higher sintering temperature the large pores become more irregular. Figure 12 and Figure 13 show the pore size distribution of SH737-2Cu and SH737-2Cu-0.9C samples for sintering temperatures of (a) 1120 °C and (b) 1180 °C.

As can be clearly seen, the maximum pores have a size below 100 μm², which is true for both sintering temperatures. From Figure 11, pore coarsening is clearly visible at higher sintering temperature (1180 °C)—the frequency of large pores (pore area of about 1500 μm²)—increases with increasing sintering temperature. Pore coarsening can also be seen in Figure 12,

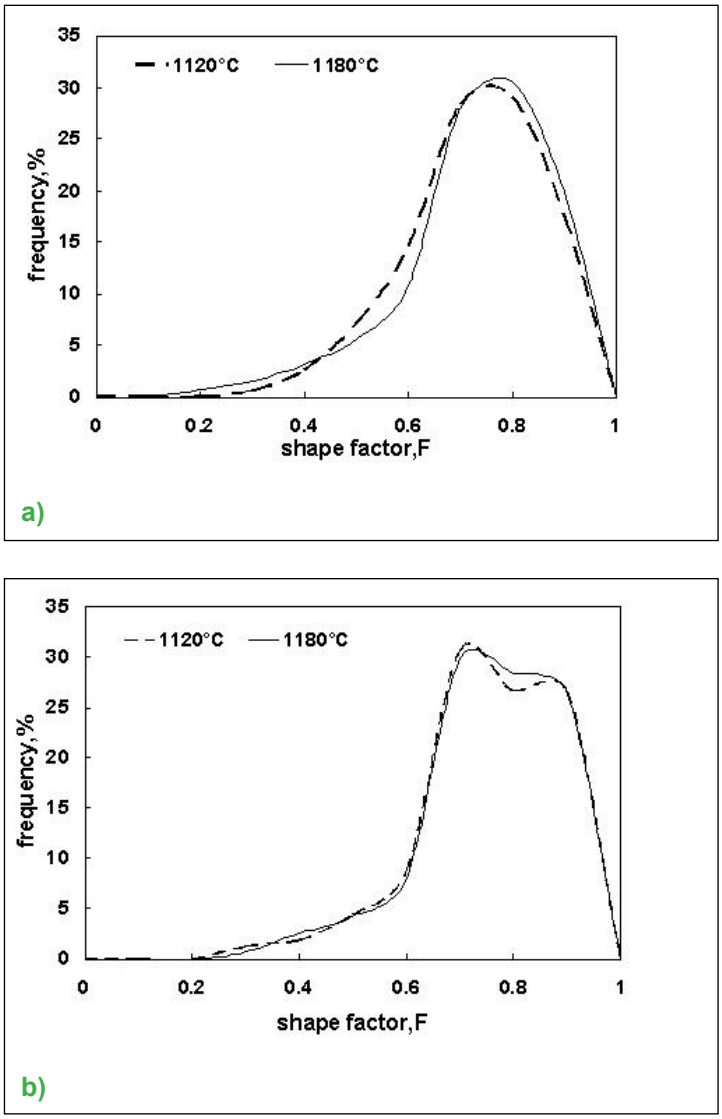

Figure 11. Variation of frequency % with shape factor of pores in samples a) SH737-2Cu and b) SH737-2Cu-0.9C at 1120 °C and 1180 °C as sintering temperatures

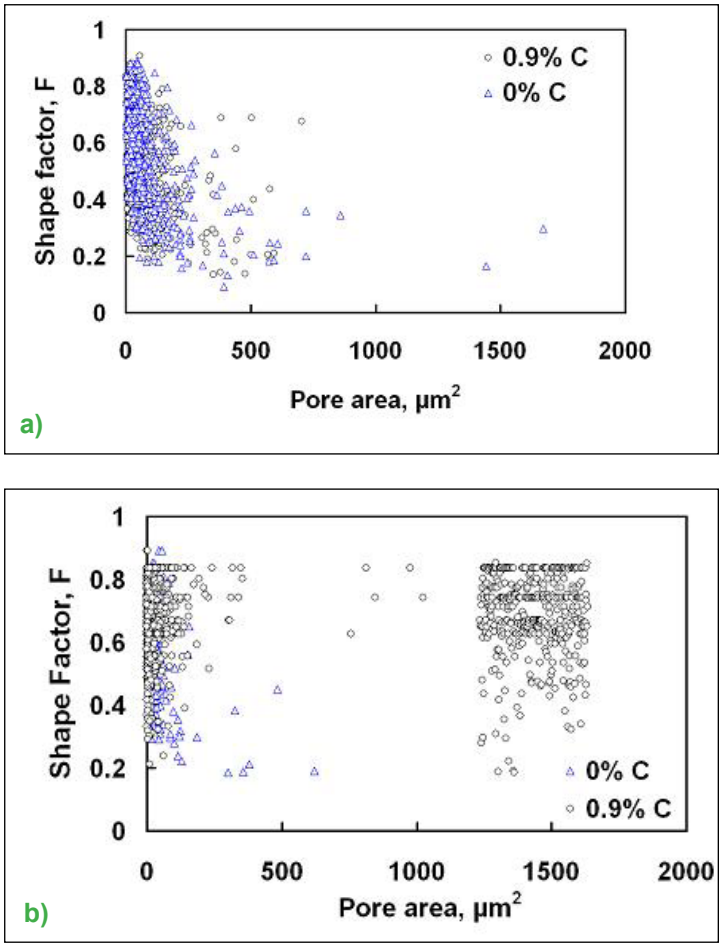

Figure 12. Variation of SF of pores with pore area of SH737-2Cu and SH737-2Cu-0.9C samples for sintering temperatures of a) 1120 °C and b) 1180 °C

which shows pore size distribution dependence on sintering temperature. Figure 13(a) and (b) show that as the sintering temperature increases, the frequency of larger pores increases and the frequency of smaller pores decreases. Pore coarsening can also be noticed in the optical microstructures shown in Figure 14.

4. Conclusions

In this study, the effect of sintering temperature and addition of carbon on the microstructure and pore morphology of a sintered alloy steel was examined. The following conclusions can be made based on the results obtained from this study:

- Carbon hinders "copper growth," preventing excessive penetration of copper rich liquid along grain boundaries or interparticle boundaries, thus reducing the swelling.
- Pore coarsening occurs in the alloy at higher sintering temperature. The average pore size increases from 7 µm to 10 µm with an increase in sintering temperature from 1120 °C to 1180 °C. At higher sintering temperature, coarser pores (> 18 µm) tend to be more irregular. However, on average, the pores tend to attain a more rounded morphology at higher sintering temperature.

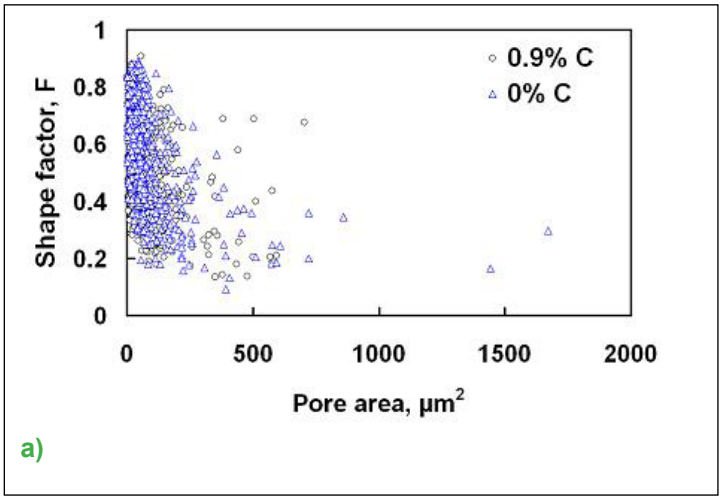

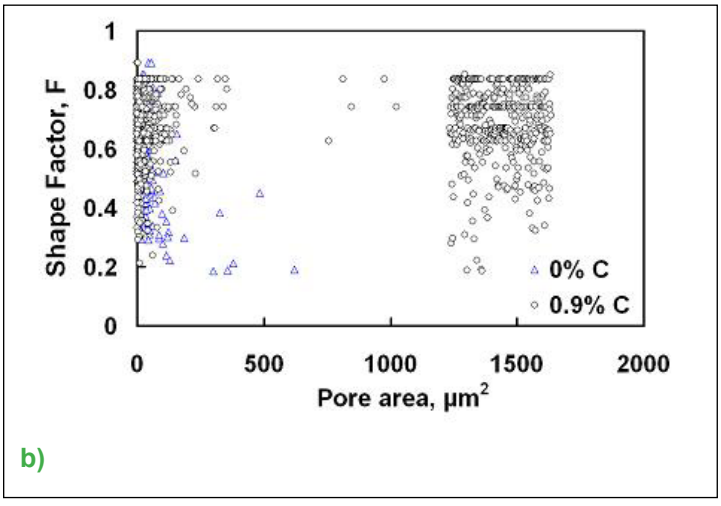

Figure 13. Pore size distribution of SH737-2Cu and SH737-2Cu-0.9C samples for sintering temperatures of a) 1120 °C and b) 1180 °C

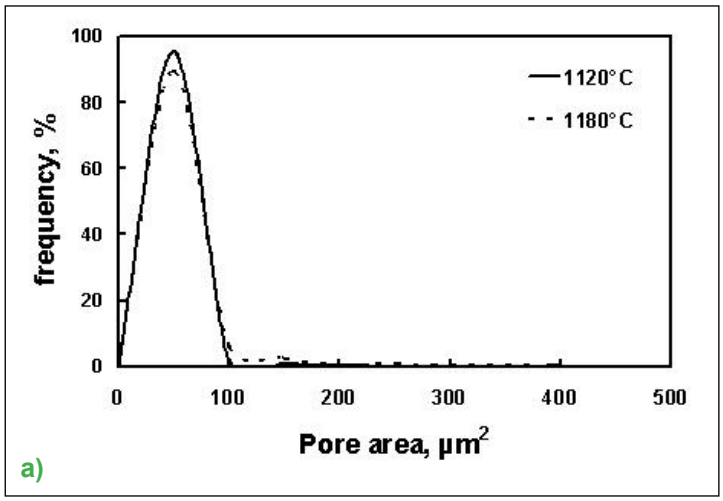

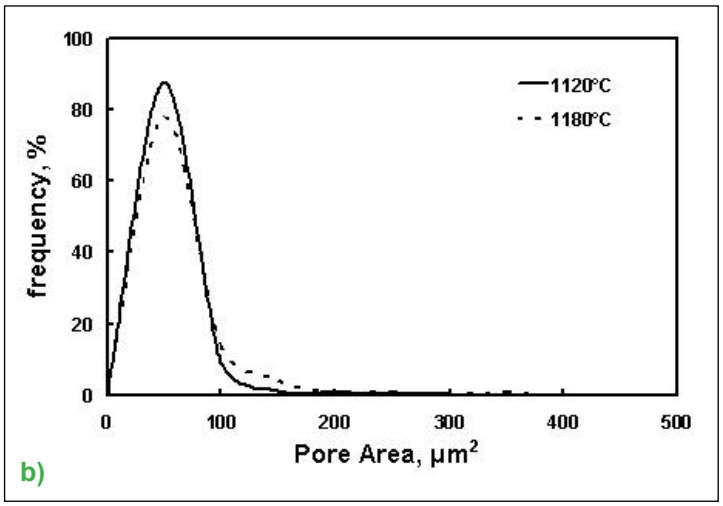

Figure 14. Effect of sintering temperature on pore size distribution for a) 0% C and b) 0.9%C

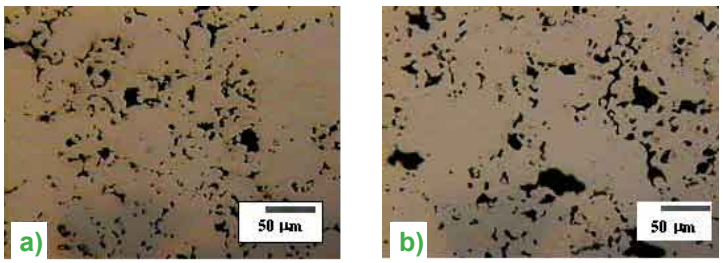

Figure 15. Optical microstructures of SH737-2Cu sintered at a) 1120 °C and b) 1180 °C showing pore coarsening occurring at higher sintering temperatures

- A bimodal SF distribution was obtained in the case of no carbon addition, primarily due to the presence of both types of pores, namely primary and secondary.

Acknowledgments

The authors gratefully acknowledge Dr. Anish Upadhyaya, Associate Professor, Department of Metallurgical and Materials Engineering, IIT Kanpur, for his supervision and Dr. Narasimhan from Hoeganaes Corporation for providing us with the working powders and for his suggestions and support.

References

[1] Upadhyaya, G. S. *Sintered Metallic and Ceramic Materials Preparation, Properties and Applications*. J. Wiley & Sons: New York, NY, USA, 1999; Vol. 1,

[2] Durdallar, C. The Effect of Additions of Cu, Ni and C on the Sintered Properties of Iron-Base Sintered P/M Parts. *Progress in Powder Metallurgy* **1969**, *25*, 73.

[3] Lenel, F. V.; Hwang, K. The Mechanical Properties of High Density Iron-Copper Alloys from a Composite Powder. *Powder Metallurgy Internationals* **1980**, *12*(20), 89.

[4] Krantz, T. Effect of Density and Composition on the Dimensional Stability and Strength of Iron-Copper Alloys. *International Journal of Powder Metallurgy* **1969**, 5(3), 35.

[5] Trudel, Y.; Angers, R. Properties of Iron-Copper Alloys made from Elemental or Prealloyed Powders. International *Journal of Powder Metallurgy and Powder Technology* **1975**, *11*(1), 5.

[6] Berner, D.; et. al. Swelling of Iron-Copper Mixtures during Sintering and Infiltration. *Modern Developments in Powder Metallurgy* **1973**, *6*, 237.

[7] Tabeshfar, K.; Chadwick, G. A. Dimensional Changes During Liquid Phase Sintering of Fe-Cu compacts. *Powder Metallurgy* **1984**, *27*(1), 19.

[8] Jamil, S. J.; Chadwick, G. A. Investigation and Analysis of Liquid Phase Sintering of Fe-Cu and Fe-Cu-C compacts. *Powder Metallurgy* **1985**, *33*(2), 65.

[9] Lawcock, R. L.; Davies, T.A. Effect of carbon on Dimensional and Microstructural Characteristics of Fe-Cu compacts during sintering. *Powder Metallurgy 1990*, *33*(2), 147.

[10] Brian James, W. *International Journal of Powder Metallurgy and Powder Technology* **1985**, *21*(2), 163.

[11] Karlsson, B.; Bertilsson, I. Scand. *Journal of Metallurgy* **1982**, *11*, 267.

[12] Salak, A.; Miskovic, V.; Dudrova, E.; Rudnayova, E. *Powder Metallurgy International* **1974**, *6*, 128.

[13] Kreher, W.; Siegel, S.; Tecza, W. *Proc Int. PM Conf. DDR, Dresden*, **1977**, *1*, 13.

[14] Haynes, R. *The Mechanical Behaviour of Sintered Metals*; Freund Publishers: London, 1981.

[15] Danninger, H. *Powder Metallurgy International* **1987**, *19*, 1.

[16] Cimino, T. M.; Graham, A. H.; Murphy, T. F. *Industrial Heating* **2000**, *September*.

[17] Christian, K. D.; German, R. M. *International Journal of Metallurgy* **1995**, *31*, 1.

[18] Chawla, N.; Fillari, G.; Narasimhan, K. S. in *Powder Materials: Current Research and Industrial Practices*. F.D.S. Marquis. Ed. TMS: Warrendale, PA, 1999; pp 247.

[19] Luk, S. H.; Hamill. Jr., J. A. *Advances in Powder Metallurgy and Particulate Materials*. Metal Powder Industries Federation: Princeton. NJ, 1993 ; pp 153.

[20] Kulu, P.; Tümanok, A.; Mikli, V.; Käerdi, H.; Kohutek, I.; Besterci, M. Possibilities of Evolution of Powder particle granulometry and morphology by image analysis. *Proc. Estonian Acad. Sci. Eng.* **1998**, *4*, 3.

[21] Saltykov, S. A. *Stereometric Metallography*. Metallurgiya, Moscow, 1976 (in Russian).

About the Authors

Neerav Verma

Neerav Verma is a senior undergraduate student of Materials and Metallurgical engineering in Indian Institute of Technology, Kanpur, India. The versatile field of Material science has always captivated him and the research areas in it have inspired him to explore them and ameliorate his knowledge to come up with decent research work. He has been involved in a rigorous research work in the field of Powder Metallurgy which included "Investigation Of Densification And Microstructural Evolution Of Sinter-Hardening Alloy Steels." He has also worked in the field of characterization of Construction Materials during his 2006 summer internship at LMC Lab, EPFL, Lausanne, Switzerland.

Saurabh Anand

Mr. Anand is currently pursuing his degree from the Department of Materials and Metallurgical Engineering at the Indian Institute of Technology, Kanpur. He has always been fascinated by the practical application of intellectual and conceptual knowledge. Recently, he has become absorbed in empirical works on powder metallurgy. Saurabh worked on a paid research project on sintered hardened grades of steel powders which included investigation of its densification, mechanical properties, and microstructural evolution. He recently completed a summer internship in an exchange program by the Australian government working on "Nanostructured Materials and Materials with Inhomogeneous Microstructure."